


Criticality of quantum energy teleportation at phase transition points in quantum field theory

Kazuki Ikeda (池田一毅)^{*}

*Department of Physics and Astronomy, Co-design Center for Quantum Advantage,
Stony Brook University, Stony Brook, New York 11794-3800, USA
and Department of Physics and Astronomy, Center for Nuclear Theory, Stony Brook University,
Stony Brook, New York 11794-3800, USA*

 (Received 31 January 2023; accepted 30 March 2023; published 17 April 2023)

Quantum field theory can be a new medium for communication through quantum energy teleportation. We perform a demonstration of quantum energy teleportation with a relativistic fermionic field theory of self-coupled fermions, called the massive Thirring model. Our results reveal that there is a close relationship between the amount of energy teleported and the phase diagram of the theory. In particular, we show that the teleported energy peaks near the phase transition points. Since these results are obtained by measuring the two local subsystems, the noise from the quantum computation can be considerably reduced, allowing for efficient quantum simulations. Moreover, it is a new entanglement-based method that reveals global structure through local measurements.

DOI: [10.1103/PhysRevD.107.L071502](https://doi.org/10.1103/PhysRevD.107.L071502)

I. INTRODUCTION

Quantum field theory (QFT) has been quite successful in explaining quantum many-body systems. From condensed matter physics, such as superconductors and topological insulators, to the standard model of elementary particles as a low-energy effective theory of high-energy physics, QFT can explain a wide variety of experimental results with extremely high precision. The approach to nonperturbative phenomena is a remaining challenge for QFT, which has been explored by various methods such as first-principles calculations and lattice QCD. In addition, with the advent of quantum computers, we are able to perform real-time nonperturbative quantum simulations of many-body systems. One of the key challenges in studying QFT is the complexity of the calculations involved. Simulating these systems using classical computers can be computationally expensive, as the complexity of the calculations increases rapidly with the size of the system. Quantum computers, on the other hand, have the potential to perform these simulations much more efficiently. In addition, the development of quantum algorithms and quantum computers has greatly contributed to the fundamental understanding of quantum mechanics, including the control of quantum states and the measurement of quantum states.

As such, understanding the behavior of quantum many-body systems through quantum simulations has been the primary focus of the recent cross-disciplinary interest in physics and computer science, but for physics, the connection with quantum science and technology is not limited to quantum computation. Regarding the connection between QFT and quantum information theory, there are active studies on entanglement entropy and black holes [1–3]. These studies are mainly concerned with high-energy physics at the Planck scale. While such attempts have been extremely successful, new efforts to reveal the nature of quantum systems and spacetime through measurement have been active in recent years in a wide range of fields, including high-energy physics, condensed matter physics, and quantum computation [4–9].

Quantum energy teleportation (QET) is a protocol for the study of local energies that takes advantage of the entanglement nature of the ground state of quantum many-body systems [10–18]. Just as quantum teleportation can transfer quantum states to remote locations [19–23], it is expected that QET can transfer energy to remote locations using local operation and classical communication (LOCC) only. The role of QET in physics and information engineering is largely unexplored, as the theory has not received much attention for a long time since it was proposed about 15 years ago. An interesting property of QET is that multiple people in different locations who share the same ground state initially can simultaneously lower the energy of their local systems by applying conditional operations. This is only possible when the sender and receivers of the energy conduct the appropriate

^{*}kazuki7131@gmail.com; kazuki.ikeda@stonybrook.edu

Published by the American Physical Society under the terms of the [Creative Commons Attribution 4.0 International license](https://creativecommons.org/licenses/by/4.0/). Further distribution of this work must maintain attribution to the author(s) and the published article's title, journal citation, and DOI. Funded by SCOAP³.

LOCC and cannot be obtained by any unitary operation or random conditional operations. (To explain this better, I disclosed the code used for quantum simulation of QET with an IBM quantum computer [17]. The code is available on both GitHub and Google Colab [24].) Therefore, QET will not only help enhance our understanding of fundamental issues in quantum statistical mechanics, condensed matter physics, and high-energy physics, but it will also provide interesting perspectives for engineering applications of quantum computation and quantum communication.

The purpose of this Letter is to investigate the role and properties of QET in field theory. From the viewpoint of quantum computer applications, we simulate QET using the massive Thirring model [low-dimensional quantum electrodynamics (QED)], which is one of the most widely used $(1+1)$ -dimensional models of QFT. First, we estimate the phase diagram of the massive Thirring model using entanglement entropy and chiral condensate. The main result of this Letter is the identification of a sharp peak in teleported energy near the phase transition point. We also analyze the time evolution of the entanglement entropy difference ΔS_{AB} using Alice's postmeasurement state and show numerically how the entanglement entropy lost in Alice's measurement is recovered over time due to particle-particle interactions in the system if Bob does nothing after Alice's measurement. Some of the results in this Letter are based on simulations of quantum gate operations using the `Qasm_Simulator` provided by IBM, and we confirm that all of these results are fully consistent with those obtained by exact diagonalization. These results provide new insights into local operations of quantum fields based on remote communication and nontrivial energy flow mediated by many-body quantum systems.

II. LOW-DIMENSIONAL QFT

The $(1+1)$ -dimensional QFTs are of significant interest since they are simpler and more tractable than higher-dimensional QFT, and they have rich mathematical structures that have been studied extensively from various motivations, including condensed matter physics, high-energy physics, statistical mechanics, and mathematical physics [25]. Some of the models have a number of interesting properties, including confinement and the chiral anomaly; therefore, they are useful toy models of QCD. The typical models preferred in studies of $(1+1)$ -dimensional QFTs are the Thirring model and the Schwinger model. In particular, they are attractive models in terms of quantum simulation and quantum computation [26–32].

The Thirring model is a simplified version of QED in $(1+1)$ dimensions, which was introduced by Walter Thirring in 1958 [33]. It is a theory of a self-coupled Dirac field, and it can be used to describe a variety of physical systems, such as superconductors [34], statistical mechanics, high-energy physics, and mathematical physics [35].

While the Thirring model and the Schwinger model are models for fermions, there is a significant $(1+1)$ -dimensional model for bosons called the sine-Gordon model, which is of significant interest in theoretical physics due to its integrability, soliton solutions, and relations to other models such as the Thirring model, massive Schwinger model, and the XY model. The sine-Gordon model is a $(1+1)$ -dimensional field theory that is described by the sine-Gordon equation, which is a non-linear partial differential equation. The soliton solution of this model describes a kink or antikink solution which is a topological mode in the field that can be interpreted as particlelike excitation [36]. The topological nature of the solitons ensures the stability, and the solitons retain their shape even during collision.

It has been widely known that both models are related by the bosonization. By representing the fermionic fields in terms of bosonic fields, the bosonized version of the Thirring model becomes the sine-Gordon model. This is known as the S duality between the two models. More detailed theoretical descriptions are given in the Supplemental Material [37].

Throughout this work, we consider the massive Thirring model, whose Lagrangian is

$$\mathcal{L}_{\text{Th}} = \bar{\psi}(i\gamma^\mu \partial_\mu - m)\psi - \frac{g}{2}\bar{\psi}\gamma^\mu\psi\bar{\psi}\gamma_\mu\psi, \quad (1)$$

where m is the fermion mass, g is the dimensionless four-fermion coupling constant, and $\psi = \psi(x)$ is a spinor field with two components $\psi_1(x)$ and $\psi_2(x)$. It is widely known that the massive Thirring model is dual to the sine-Gordon model and the classical two-dimensional XY model [38]. For example, a Kosterlitz-Thouless phase transition at $T \sim K\pi/2$ in the XY model corresponds to a critical point $g \sim -\pi/2$ called Coleman's instability point in the Thirring model. They are also related to a critical point at $t \sim 8\pi$ in the sine-Gordon model.

It turns out that the spin representation of the massive Thirring model is

$$H_{\text{Th}} = -\frac{1}{4a} \sum_{n=0}^{N-2} (X_n X_{n+1} + Y_n Y_{n+1}) + \frac{m}{2} \sum_{n=0}^N (-1)^{n+1} Z_n + \frac{\Delta(g)}{a} \sum_{n=0}^{N-2} \left(\frac{Z_n + 1}{2}\right) \left(\frac{Z_{n+1} + 1}{2}\right), \quad (2)$$

where $\Delta(g) = \cos(\frac{\pi-g}{2})$, and a is the lattice spacing [38–43]. The theoretical background of the lattice Hamiltonian is described in the Supplemental Material [37]. Note that only mass m and lattice spacing a have mass dimension, and ma is a dimensionless parameter. We take $\hbar = 1$.

III. SIMULATION OF QUANTUM ENERGY TELEPORTATION

To facilitate clarity of the results, we add a constant ϵ_i to every local Hamiltonian of the Thirring model

$$H_{\text{Th}} = \sum_n H_n, \quad (3)$$

where H_n is the local Hamiltonian including the nearest-neighbor interactions, and each ϵ_n should be chosen in such a way that

$$\langle g|H_{\text{Th}}|g\rangle = \langle g|H_n|g\rangle = 0, \quad \forall i \in E, \quad (4)$$

where $|g\rangle$ is the ground state of the total Hamiltonian H_{Th} . Note that, in general, $|g\rangle$ is not the ground state of local H_n . The explicit form of Bob's local Hamiltonian and the details of computation are given in Supplemental Material [37] Eq. (A9). It is important that nontrivial local manipulations, including the measurement of the ground state, yield excited states and thus increase the energy expectation value. The increase in energy is supplied by the experimental apparatus. Moreover, our ground state $|g\rangle$ is an entangled state in general.

The QET protocol is as follows. First, Alice measures her Pauli operator σ_{n_A} by $P_{n_A}(\mu) = \frac{1}{2}(1 + \mu\sigma_{n_A})$ and obtains either $\mu = -1$ or $+1$. The local measurement of the quantum state at a subsystem A destroys this ground state entanglement. At the same time, energy E_A from the device making the measurement is injected into the entire system. The injected energy E_A is localized around the subsystem A in the very early stages of time evolution; however, it is not possible for Alice to extract E_A from the system by her operations alone at n_A . This is because information about E_A is also stored in remote locations other than n_A due to the entanglement that exists prior to the measurement. In other

words, Alice's energy E_A can be partially extracted at any location other than n_A . Now let us consider taking advantage of the quantum many-body nature of the quantum many-body system to extract energy from a different location other than n_A . This can be accomplished by LOCC, as shown below.

Via a classical channel, Alice sends her measurement result μ to Bob, who applies an operation $U_{n_B}(\mu)$ to his qubit and measures his local operators $X_{n_B}, Y_{n_B}, Z_{n_B}$ independently. The density matrix ρ_{QET} after Bob operates $U_{n_B}(\mu)$ to $P_{n_A}(\mu)|g\rangle$ is where ρ_{QET} is

$$\rho_{\text{QET}} = \sum_{\mu \in \{-1,1\}} U_{n_B}(\mu) P_{n_A}(\mu) |g\rangle \langle g| P_{n_A}(\mu) U_{n_B}^\dagger(\mu). \quad (5)$$

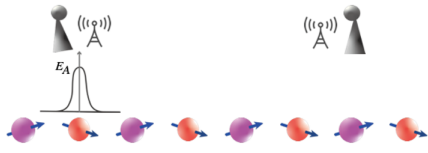
Using ρ_{QET} , the expected local energy at Bob's local system is evaluated as $\langle E_{n_B} \rangle = \text{Tr}[\rho_{\text{QET}} H_{n_B}]$, which is negative in general. Because of the conservation of energy, $E_B = -\langle E_{n_B} \rangle (> 0)$ is extracted from the system by the device that operates $U_{n_B}(\mu)$ [44]. In this way, Alice and Bob can transfer the energy of the quantum system only by operations on their own LOCC. These are summarized in Fig. 1.

It should be noted that the Thirring model is a relativistic field theory in performing QET, which could be a problem if the particle is massless since the speed of classical communication does not exceed the speed of light. We will consider a massive particle and assume that Bob can receive energy faster than the time-evolution rate of the system.

In what follows, we give the details about the operations of Alice and Bob. We define $U_{n_B}(\mu)$ by

$$U_{n_B}(\mu) = \cos \theta I - i\mu \sin \theta \sigma_{n_B}, \quad (6)$$

(1) Alice measures her qubit and tells the result to Bob by a classical channel



(2) Bob applies conditional operation(s) to receive energy

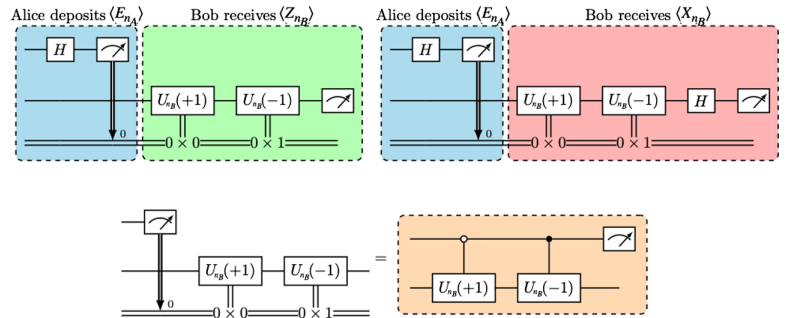
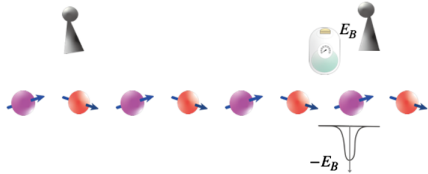


FIG. 1. Protocol of quantum energy teleportation (left) and the corresponding quantum circuits (right). First, Alice measures her local operator X_{n_A} and tells her result ($\mu \in \{+1, -1\}$) to Bob. At this point, Alice's local energy is excited $E_{n_A} > 0$. Then, to obtain energy, Bob applies conditional operation $U_{n_B}(\mu)$ to his local qubit and measures the corresponding terms of his local Hamiltonian H_{n_B} . Statistically, he will observe $\langle H_{n_B} \rangle = \text{Tr}[\rho_{\text{QET}} H_{n_B}] < 0$ and gain $E_{n_B} = -\langle H_{n_B} \rangle$ through his measurement device.

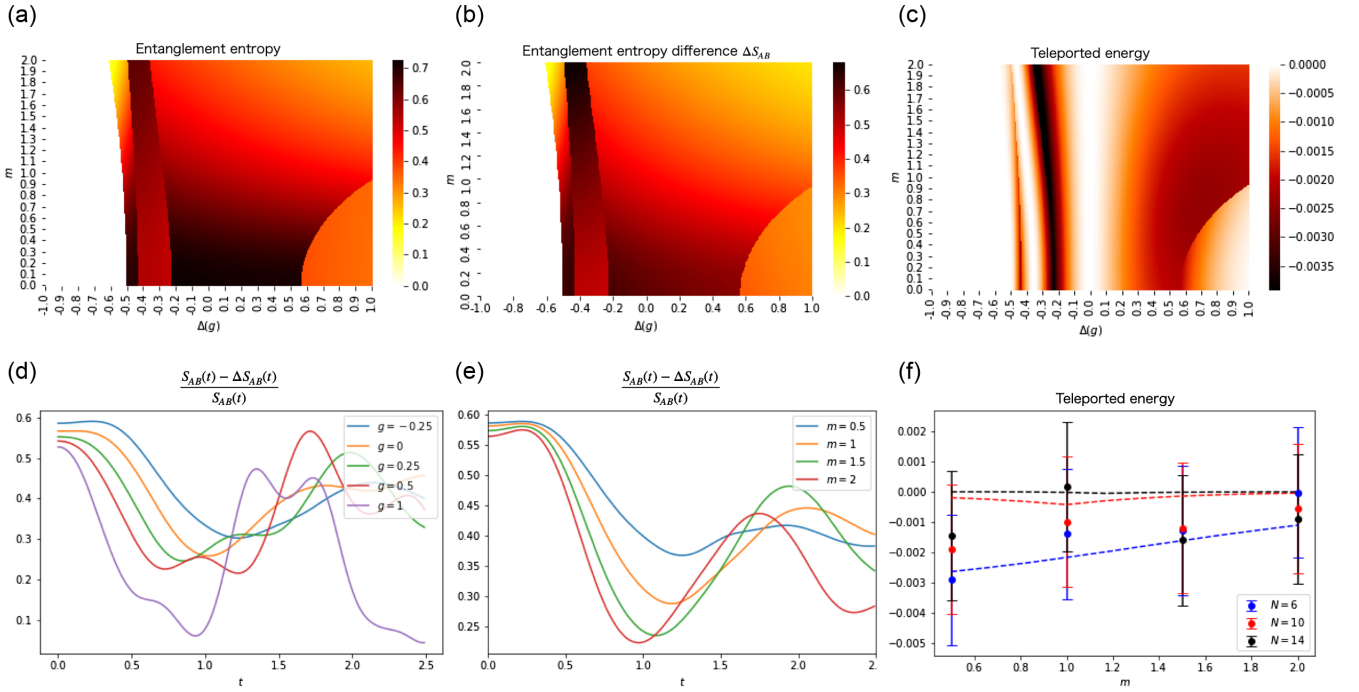


FIG. 2. (a) Heat map of entanglement entropy at $N = 6$. The Thirring model has three distinct phases, which can be clearly read off the diagram at $N = 6$. (b) Heat map of entanglement entropy difference ΔS_{AB} . (c) Heat map of teleported energy $\langle H_{n_B} \rangle$ at $N = 6$. It is crucial that the value of the teleported energy peaks at the phase transition points, showing a clear correspondence to the phase diagram. (d),(e) Time evolution of the entanglement entropy difference. This is due to the natural time evolution of the system, as seen when Bob does not perform any operations on his system after Alice's local operations. Decreasing $1 - \frac{\Delta S_{AB}}{S_{AB}}$ in the early stages of time evolution means that entanglements broken by Alice's observations are recreated by the interactions in the system. (f) Simulation results of expected energy of Bob's local system obtained by QET. Error bars indicate statistical errors.

where θ obeys

$$\cos(2\theta) = \frac{\xi}{\sqrt{\xi^2 + \eta^2}}, \quad (7)$$

$$\sin(2\theta) = -\frac{\eta}{\sqrt{\xi^2 + \eta^2}}, \quad (8)$$

where

$$\xi = \langle g | \sigma_{n_B} H \sigma_{n_B} | g \rangle, \quad (9)$$

$$\eta = \langle g | \sigma_{n_A} \dot{\sigma}_{n_B} | g \rangle \quad (10)$$

with $\dot{\sigma}_{n_B} = i[H, \sigma_{n_B}]$. The local Hamiltonian should be chosen so that $[H, \sigma_{n_B}] = [H_{n_B}, \sigma_{n_B}]$. The average quantum state ρ_{QET} is obtained after Bob operates $U_{n_B}(\mu)$ on $P_{n_A}(\mu)|g\rangle$. Then, the average energy Bob measures is

$$\langle E_{n_B} \rangle = \text{Tr}[\rho_{\text{QET}} H_{n_B}] = \frac{1}{2} \left[\xi - \sqrt{\xi^2 + \eta^2} \right], \quad (11)$$

which is negative if $\eta \neq 0$. If there is no energy dissipation, the positive energy of $-\langle E_{n_B} \rangle$ is transferred to Bob's device after the measurement due to energy conservation. Based on

the quantum circuit in Fig. 1, we performed a quantum simulation of QET for $N = 6, 10, 14$ at $\Delta(g) = -0.2$, $a = 0.2$, and the results are shown in Fig. 2(f). Dashed lines correspond to the exact results. In this work, we put Alice and Bob near the boundary $n_A = 1, n_B = N - 2$. Bob's local energy can be calculated by the explicit form of his local Hamiltonian given in Eq. (A9) in the Supplemental Material [37]. The simulation results are given in Table I in the Supplemental Material [37].

Here let us describe the importance of the results. First, the efficiency of this work can be explained as follows. First of all, in general, to measure physical quantities in a quantum many-body system using a quantum computer, it is customary to measure all the qubits. However, the measurement of each qubit is accompanied by noise, making it extremely difficult to accurately measure physical quantities in large systems. Given that error correction also requires a huge number of qubits, it is not realistic to measure all qubits accurately. In contrast, the method using energy teleportation reproduces the basic structure of the phase diagram by measuring only the six terms of the local Hamiltonian (as shown in Table I in the Supplemental Material [37]), regardless of the system size (see also Fig. 1 in the Supplemental Material [37]). This dramatically improves computational efficiency.

Additionally, it is extremely nontrivial that long-range correlations can be captured by measuring only two points. This is because the overall structure is not determined solely by local properties. Our results provide an affirmative and explicit solution to this nontrivial question by using entanglement in the ground state of quantum many-body systems. This result will have major implications for experiments and measurements of quantum many-body systems. In fact, similar reports are provided in symmetry-protected topological materials and the Ising model [45].

We next study the entanglement entropy between two subsystems A, B such that $A \cap B = \emptyset, A \cup B = \{1, 2, \dots, N\}$. It is known that entanglement entropy is a good order parameter in spin chains [46]. Let ρ be a density operator on the entire system $A \cup B$. Then, the entanglement entropy between A and B is defined by

$$S(\rho) = -\text{Tr}_A(\rho_A \log \rho_A), \quad (12)$$

where ρ_A is defined by tracing out the Hilbert space of B : $\rho_A = \text{Tr}_B \rho$. In this study, we choose ρ as the ground state $|g\rangle$ of the Hamiltonian ($\rho = |g\rangle\langle g|$). Figure 2(a) shows the entanglement entropy between the left and right half subsystems, i.e., $A = \{0, \dots, \frac{N}{2}\}$. The figure exhibits sharp peaks at the critical points of phase transitions that can be understood by the phase diagram of chiral condensate in Fig. 1 in the Supplemental Material [37]. Figure 2(c) shows the teleported energy $\text{Tr}[\rho_{\text{QET}} H_{n_B}]$ to Bob's local system. It is significant that the teleported energy is enhanced along the critical points of the phase transition. This will be understood by a relation between Bob's energy $\text{Tr}[\rho_{\text{QET}} H_{n_B}]$ and the entanglement entropy difference ΔS_{SA} , which is shown in Fig. 2(b).

The change in entropy before and after the measurement by Alice can be evaluated as follows:

$$\Delta S_{AB} = S_{AB} - \sum_{\mu} p_{\mu} S_{AB}(\mu), \quad (13)$$

where p_{μ} is the probability distribution of μ , and $S_{AB}(\mu)$ is the entanglement entropy after the measurement $\xi = \arctan(\frac{\xi}{\hbar})$. After Alice's postmeasurement, the state is mapped to

$$|A(\mu)\rangle = \frac{1}{\sqrt{P_{\mu}}} P_{n_A}(\mu) |g\rangle. \quad (14)$$

Then, $S_{AB}(\mu)$ is calculated with the density matrix $|A(\mu)\rangle\langle A(\mu)|$.

As discussed in Refs. [11,47], ΔS_{AB} is bounded below by a function $f(\xi, \eta)$ in such a way that

$$\Delta S_{AB} \geq f(\xi, \eta) E_B. \quad (15)$$

This indicates that the transferring energy involves a commensurate consumption of entropy. Similar to the Maxwell demon argument [48,49], Bob's conditional operations reduce the entropy of the local system. If Bob does nothing after Alice's measurement, Figs. 2(d) and 2(e) illustrate how the entanglement entropy is re-created by the natural time evolution of the system. Moreover, the maximal energy that Bob would receive is bounded below by the difference in entropy:

$$\max_{U_1(\mu)} E_B \geq h(\xi, \eta) \Delta S_{AB}, \quad (16)$$

where $h(\xi, \eta)$ is a certain function.

Although it is difficult to analytically obtain the concrete forms of functions f and h , the results of this study show that there is a clear correspondence between the energy obtained by QET and the phase diagram of QFT.

ACKNOWLEDGMENTS

I thank Adrien Florio, David Frenklakh, Sebastian Griener, Fangcheng He, Masahiro Hotta, Dmitri Kharzeev, Yuta Kikuchi, Vladimir Korepin, Qiang Li, Adam Lowe, René Meyer, Shuzhe Shi, Hiroki Sueno, Tzu-Chieh Wei, Kwangmin Yu, and Ismail Zahed for fruitful communication and collaboration. I thank Megumi Ikeda for providing the illustrations. I acknowledge the use of IBM quantum computers and simulators. I was supported by the U.S. Department of Energy, Office of Science, National Quantum Information Science Research Centers, Co-design Center for Quantum Advantage under Contract No. DESC0012704.

All work was performed by the author.

The author declares that there is no competing financial interest.

- [1] S. Ryu and T. Takayanagi, *Phys. Rev. Lett.* **96**, 181602 (2006).
- [2] B. Yoshida, *J. High Energy Phys.* **10** (2019) 132.
- [3] P. Hayden and J. Preskill, *J. High Energy Phys.* **09** (2007) 120.
- [4] T. Minato, K. Sugimoto, T. Kuwahara, and K. Saito, *Phys. Rev. Lett.* **128**, 010603 (2022).
- [5] T. Hashizume, G. Bentsen, and A. J. Daley, *Phys. Rev. Res.* **4**, 013174 (2022).
- [6] H. J. Briegel, D. E. Browne, W. Dür, R. Raussendorf, and M. Van den Nest, *Nat. Phys.* **5**, 19 (2009).
- [7] V. Gebhart, K. Snizhko, T. Wellens, A. Buchleitner, A. Romito, and Y. Gefen, *Proc. Natl. Acad. Sci. U.S.A.* **117**, 5706 (2020).
- [8] D. T. Stephen, W. W. Ho, T.-C. Wei, R. Raussendorf, and R. Verresen, *arXiv:2209.06191*.
- [9] J. M. Koh, S.-N. Sun, M. Motta, and A. J. Minnich, *arXiv:2203.04338*.
- [10] M. Hotta, *Phys. Lett. A* **372**, 5671 (2008).
- [11] M. Hotta, *J. Phys. Soc. Jpn.* **78**, 034001 (2009).
- [12] J. Trevison and M. Hotta, *J. Phys. A* **48**, 175302 (2015).
- [13] M. Hotta, *Phys. Rev. A* **80**, 042323 (2009).
- [14] Y. Nambu and M. Hotta, *Phys. Rev. A* **82**, 042329 (2010).
- [15] M. Hotta, *J. Phys. A* **43**, 105305 (2010).
- [16] N. A. Rodríguez-Briones, H. Katiyar, R. Laflamme, and E. Martín-Martínez, *Phys. Rev. Lett.* **130**, 110801 (2023).
- [17] K. Ikeda, *arXiv:2301.02666*.
- [18] K. Ikeda, *arXiv:2301.11884*.
- [19] C. H. Bennett, G. Brassard, C. Crépeau, R. Jozsa, A. Peres, and W. K. Wootters, *Phys. Rev. Lett.* **70**, 1895 (1993).
- [20] A. Furusawa, J. L. Sørensen, S. L. Braunstein, C. A. Fuchs, H. J. Kimble, and E. S. Polzik, *Science* **282**, 706 (1998).
- [21] S. Pirandola, J. Eisert, C. Weedbrook, A. Furusawa, and S. L. Braunstein, *Nat. Photonics* **9**, 641 (2015).
- [22] S. Takeda, T. Mizuta, M. Fuwa, P. Van Loock, and A. Furusawa, *Nature (London)* **500**, 315 (2013).
- [23] B. Thotakura and T.-C. Wei, *arXiv:2209.07021*.
- [24] K. Ikeda, Quantum Energy Teleportation with Quantum Computers (2023), <https://github.com/IKEDAKAZUKI/Quantum-Energy-Teleportation.git>.
- [25] A. Izergin and V. Korepin, *Nucl. Phys.* **B205**, 401 (1982).
- [26] K. Ikeda, D. E. Kharzeev, and Y. Kikuchi, *Phys. Rev. D* **103**, L071502 (2021).
- [27] M. Honda, E. Itou, Y. Kikuchi, and Y. Tanizaki, *Prog. Theor. Exp. Phys.* **2022**, 033B01 (2022).
- [28] D. E. Kharzeev and Y. Kikuchi, *Phys. Rev. Res.* **2**, 023342 (2020).
- [29] B. Chakraborty, M. Honda, T. Izubuchi, Y. Kikuchi, and A. Tomiya, *Phys. Rev. D* **105**, 094503 (2022).
- [30] C. Mishra, S. Thompson, R. Pooser, and G. Siopsis, *Quantum Sci. Technol.* **5**, 035010 (2020).
- [31] N. Klco, E. F. Dumitrescu, A. J. McCaskey, T. D. Morris, R. C. Pooser, M. Sanz, E. Solano, P. Lougovski, and M. J. Savage, *Phys. Rev. A* **98**, 032331 (2018).
- [32] A. Florio, D. Frenklakh, K. Ikeda, D. Kharzeev, V. Korepin, S. Shi, and K. Yu, *arXiv:2301.11991*.
- [33] W. E. Thirring, *Ann. Phys. (N.Y.)* **3**, 91 (1958).
- [34] M. Faber and A. N. Ivanov, *Eur. Phys. J. C* **20**, 723 (2001).
- [35] V. E. Korepin, *Teor. Mat. Fiz.* **41**, 169 (1979).
- [36] L. Faddeev and V. Korepin, *Phys. Rep.* **42**, 1 (1978).
- [37] See Supplemental Material at <http://link.aps.org/supplemental/10.1103/PhysRevD.107.L071502> for the complete data table of quantum energy teleportation, details of quantum operations, theoretical background, and adiabatic state preparation of the massive Thirring model.
- [38] S. Mandelstam, *Phys. Rev. D* **11**, 3026 (1975).
- [39] A. Luther, *Phys. Rev. B* **14**, 2153 (1976).
- [40] S. Coleman, *Phys. Rev. D* **11**, 2088 (1975).
- [41] M. C. Bañuls, K. Cichy, Y. J. Kao, C. J. D. Lin, Y. P. Lin, and T. L. Tan, *arXiv:1810.12038*.
- [42] M. C. Bañuls, K. Cichy, Y.-J. Kao, C. J. D. Lin, Y.-P. Lin, and D. T. L. Tan, *Phys. Rev. D* **100**, 094504 (2019).
- [43] M. C. Bañuls, K. Cichy, Y.-J. Kao, C. J. D. Lin, Y.-P. Lin, and D. Tao-Lin Tan, *EPJ Web Conf.* **175**, 11017 (2018).
- [44] M. Hotta, *Phys. Rev. D* **78**, 045006 (2008).
- [45] K. Ikeda, *arXiv:2302.09630*.
- [46] G. Vidal, J. I. Latorre, E. Rico, and A. Kitaev, *Phys. Rev. Lett.* **90**, 227902 (2003).
- [47] M. Hotta, *arXiv:1101.3954*.
- [48] T. Sagawa and M. Ueda, *Phys. Rev. Lett.* **100**, 080403 (2008).
- [49] S. Lloyd, *Phys. Rev. A* **56**, 3374 (1997).